# Specific surface area of combustion emitted particles: Impact of primary particle diameter and organic content

François-Xavier Ouf, Soleiman Bourrous, Cécile Vallières, Jerôme Yon, Laura Lintis

Version of Record: https://www.sciencedirect.com/science/article/pii/S0021850219305324
Manuscript_0709425816a9ad2368290edf4c4038a5

# Specific surface area of combustion emitted particles: Impact of primary particle diameter and organic content

F.-X. Ouf[1], S. Bourrous[1], C. Vallières[2], J. Yon[3], and L. Lintis[1, 2]

[1]Institut de Radioprotection et de Sûreté Nucléaire (IRSN), PSN-RES, SCA, Gif-Sur-Yvette, 91192, France.

[2]Université de Lorraine, Laboratoire Réactions et Génie des Procédés (LRGP), UMR 7274, F-54000, Nancy, France.

[3]Normandie Université, INSA Rouen, UNIROUEN, CNRS, CORIA, 76000 Rouen, France.

## Abstract

Specific surface areas of particles produced at small-scale diffusion flame burners and also in pilot and large-scale fires involving complex fuels are reported and compared. Specific surface area $S_{BET}$ is determined by BET (Brunauer-Emmett-Teller) analysis and also according to previously developed approach $S_{TEM}$ relying on the primary sphere based on TEM (Tansmission Electron Microscopy) images analysis. True density is also determined and the respective influences of primary particle diameter ($D_{pp}$) and organic carbon to total carbon ratio (OC/TC) are discussed. The present study is the first to propose a careful comparison between TEM and BET specific surface areas of 20 different samples of carbonaceous particles emitted under realistic fire conditions and to bring validity range for such TEM based approach. For samples containing low and moderate OC content (less than 20%), a good agreement between $S_{TEM}$ and $S_{BET}$ is reported (within +/- 20% for a confidence interval of 95%), confirming the significant influence of primary particle diameter and the relevance of a purely geometrical description of the surface specific area of soot particles. For larger OC/TC, such approach fails to predict the particles specific surface area within a reasonable confidence interval.

## Introduction

Particles emitted in case of fire have several major impacts on fire evolution within a confined and poorly ventilated industrial facility. Considering propagation of fire, soot radiative properties are of main importance in the global radiative heat transfer within compartment fire and are now considered in fire simulation software (Cheung et al., 2004; Pierce & Moss, 2007). Such soot properties are strongly linked to their specific surface area (Michelsen et al., 2007) that is defined as the particle surface at its interface with the gas phase by mass unit. For industrial facilities handling or manufacturing hazardous materials (nuclear, biological, nanoparticles), containment of such toxic and radiotoxic materials is generally carried out according to ventilation system, aiming to keep facility in an under pressure condition, and High Efficiency Particulate Air filters (HEPA) avoiding any release within the atmosphere. In case of fire, the airflow resistance of such HEPA filters could rapidly increase and several authors have proposed empirical and semi-phenomenological models aiming to describe filters behavior in such conditions (Bourrous et al., 2016; Gregory et al., 1982; Ishibashi et al., 2014; Mocho & Ouf, 2011). Furthermore, combustion generated particles as diesel and fire emissions are well known for their toxicological impact through their composition and potential PAH (polycyclic aromatic hydrocarbons) adsorbed at their surface (Gustafsson & Gschwend, 1997; Jonker & Koelmans, 2002). Resuspended fire-emitted particles (Bolstad-Johnson et al., 2000) or direct exposure during fire training is also in debate since recent findings have highlighted the link between dustiness and mass-specific surface area of nanostructured powders (Dazon et al., 2017). Beyond all these questions, several authors have proposed experimental database describing size distribution, elemental and chemical composition (Hertzberg & Blomqvist, 2003; Motzkus et al., 2012; Ouf et al., 2015; Ouf et al., 2008; Rhodes et al., 2011; Wang et al., 2019) and more recently dealing with morphology (Bourrous et al., 2018) and true density (Ouf et al., 2019). Nevertheless, literature appears to be limited when considering specific surface area of carbon-based particles emitted during realistic fire conditions. Such surface to mass property of combustion emitted particles is of main interest since several authors have recently pointed out that specific surface area is one of the most relevant properties of nanoparticles (Schmid & Stoeger, 2016) and soot particles (Steiner et al., 2016) for characterizing their toxicity. Nevertheless, few measurements of specific surface area have been reported due to the difficulty of collecting sufficient quantities of materials for

BET analysis. In most cases, experimental data are limited to analysis of soot emitted by laboratory scale burners or aircraft engines for atmospheric applications (Popovicheva, Persiantseva, Tishkova, Shonija, & Zubareva, 2008), candles flames for producing super-hydrophobic coating (Qahtan, Gondal, Alade, & Dastageer, 2017) or diesel engines for toxicological applications (Stoeger et al., 2005). To our knowledge, present study is the first to propose a careful comparison between TEM and BET specific surface areas of carbonaceous particles emitted in case of fires.

The aim of the present paper is to review the values of specific surface area reported in the literature for soot particles (defined by Petzold et al. (2013) as agglomerates of monomers consisting solely of carbon with small amounts of hydrogen and oxygen) and to propose additional values for combustion emitted particles from materials relevant to fire emission studies at several scales and under different ventilation and dioxygen concentration conditions (also including soot particles). Reported values are obtained according to reference measurement method, i.e. BET analysis (Gregg & Sing, 1982). Influence of the organic content (OC) and primary particle diameter ($D_{pp}$) of combustion emitted particles samples are then highlighted, showing a significant decrease of specific surface area as their OC content and primary particle diameter increase. The present study demonstrates that, using previously-reported material density (Ouf et al., 2019), TEM analysis is a viable way of determining specific surface area of complex carbonaceous samples produced during fires.

## Experimental method and samples properties

Measurement of specific surface area of combustion emitted particles was carried out according to BET and using ASAP 2020 analyzer from Micromeritics©. In order to keep samples in their initial production conditions (i.e. low volatility of organic content or other condensable species formed during combustion), samples were only outgassed under primary vacuum at 298K until pressure in outgassing chamber reached stable value of 0.1 mbar (from 2 hours to nearly 12 hours depending on sample). Nitrogen adsorption measurements were conducted at 77K and the specific surface area $S_{BET}$, defined as the surface occupied by one monolayer of nitrogen molecules, is computed according to the BET approach (Sing, 1985).

In addition to BET analysis, samples were characterized in terms of primary particle diameters and organic to total carbon ratio (OC/TC), respectively by transmission electronic microscopy associated to image analysis protocol (Bourrous et al., 2018; Ouf et al., 2010) and Sunset Lab EC/OC analyzer associated to the IMPROVE_A protocol (Chow et al., 2007). True samples densities were also determined according to an experimental methodology previously described in Ouf et al. (2019).

Within the present work, combustion emitted particles were produced by different sources at different scales: analytical test bench based on miniCAST soot generator (Yon et al., 2015), cone calorimeter (Mocho & Ouf, 2011; Ouf et al., 2015; Ouf et al., 2008), large scale fires conducted within over-ventilated/open (SATURNE facility) or under-ventilated/confined (DIVA facility) conditions (Ouf et al., 2014). Liquid fuels (heptane, hydraulic oil and nuclear waste treatment solvents tributylphosphate TBP and hydrogenated tetrapropylene TPH), solid polymers composing gloves boxes used in nuclear industry for handling and manufacturing radioactive materials (polymethyl methacrylate PMMA and polyvinylchloride PVC) and electrical cables (containing significant amount of metallic elements and complex fire retardants) commonly used in many industrial facilities were considered as fuels. Fire conditions were mainly flaming and sampling points were placed at a distance of at least 10 times the exhaust duct diameters from the emission point for ensuring homogeneous aerosol concentration and representative sampling. Soot particles were mechanically or pneumatically retrieved respectively from previously clogged pleated or plane High Efficiency Particulate Air Filters implemented on ventilation network of test benches. Reference carbon black samples (Printex 90, Flamruss 101) were also considered for comparison with literature and validation of the present measurement protocol.

Physico-chemical properties of these samples are reported in Table 1. One must notice that samples produced within the present study were all characterized, in terms of physico-chemical properties, according to the same analytical methods. This careful experimental analysis allows a relevant discussion of the direct influence of those properties on specific surface area. Non-exhaustive literature analysis is also integrated in Table 1 for

carbon black and soot samples for which specific surface area, primary particle diameter and organic to total carbon ratio were available.

**Experimental results: evidence of the influence of primary particle diameter and organic carbon content**

Specific surface area of carbon black and combustion emitted particles are reported in Figure 1 as a function of primary particle diameter. Values associated to carbon black are ranging from 10 to 1000 m²/g, highlighting the large variety of samples commercially available. For particles produced under small and medium scale fire conditions (diffusion flames in figure 1), specific surface area determined by BET ($S_{BET}$) is within a narrower range from 10 to 100 m²/g, values in agreement with those reported in literature for soot emitted by gaseous burner or diesel/aircraft engines. Finally, particles emitted during realistic fire scenario (real scale fires in figure 1) are characterized by significantly lower specific surface areas (from 1 to 30 m²/g) associated to a complex composition (high OC and non-carbonaceous content, Ouf et al., 2019).

As previously reported by several authors (Bau et al., 2010; Gwaze et al., 2006; Pawlyta et al., 2018), $S_{BET}$ logically appears to be inversely dependent on $D_{pp}$. Nevertheless, one must notice discrepancies for smallest particle sizes (i.e. lower than 20 nm) and very high specific surface area. Since such discrepancies are mainly associated to carbon black samples analyzed by TEM and BET within separated studies, one could suspect slight physico-chemical differences between samples, even for commercial carbon black. Furthermore, high specific surface area (higher than 300 m²/g) of carbon black samples could only be reached by various complex after-treatments process (thermal or chemical) changing both primary particles surface rugosity and chemical composition (colour black FW200 as an example). In this case, such power-law fit, illustrated as a guide for the eye in Figure 1, is no more suitable and appears to be limited to non-porous carbon black samples and soot particles denoting low OC content. Good correlation is then reported between BET and $D_{pp}$ for soot and combustion emitted particles considered in the present study and denoting specific surface area up to 160 m²/g. For samples produced under realistic fire conditions, $S_{BET}$ appears to decrease significantly when increasing primary particle diameter, but also when increasing OC content (see Figure 1). Obviously, it appears that specific surface area does not depend only on primary particle diameter, but also on potential overlapping of those monomers within aggregates (Bau et al., 2010). Particles true density, which is highly influenced by the organic contents and significantly decreases with increasing OC/TC (Ouf et al., 2019), is also suspected to play a role (see eq. 1).

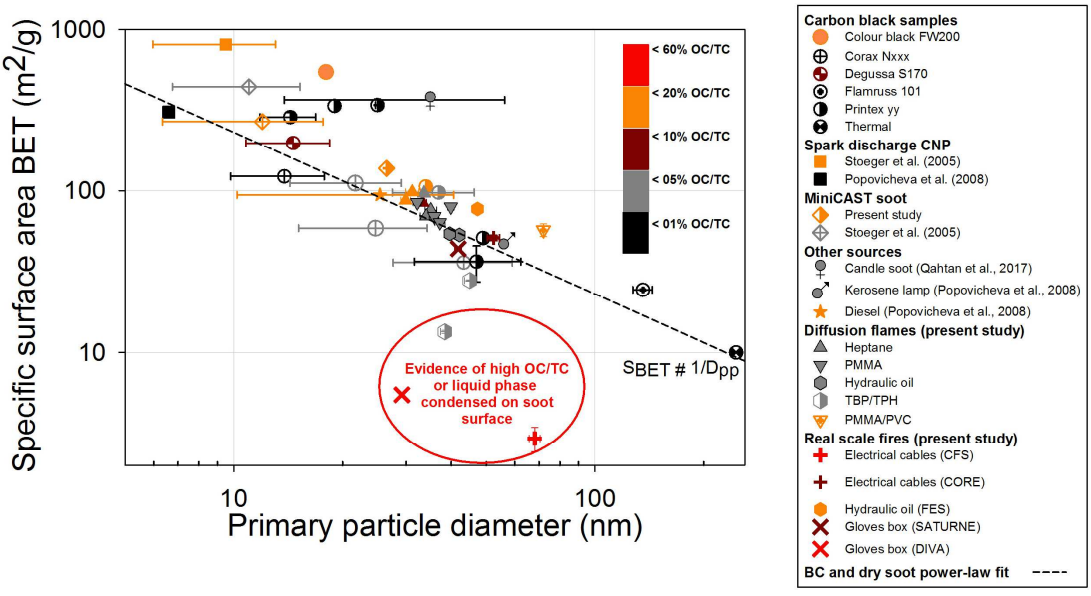


Figure 1: Evolution of soot specific surface area as a function of primary particle diameter

**Prediction of specific surface area of complex soot particles from TEM images analysis**

In order to account for the fractal morphology of nanoparticles aggregates/agglomerates (including soot, with or without overlapping), several authors have proposed empirical relations aiming to predict their specific surface area (Bau et al., 2010; Brasil, Farias, & Carvalho, 1999; Gwaze et al., 2006; Pawlyta et al., 2018). More recently, it has been proposed a quasi-automatic TEM images analyzing tool opening the way to a nanoparticles (NPs) and soot particles determination of specific surface areas in good agreement with BET analysis (Bourrous et al., 2018). For this purpose, the following relation, introduced by Bau et al. (2010), has been considered:

$$S_{TEM\ Bau}=\frac{6}{\rho_{pp}}\left[1-\Phi Cov\left(1-\frac{1}{N_{pp}}\right)\right]\frac{\sum_{D_{pp}}N(D_{pp})D_{pp}^{2}}{\sum_{D_{pp}}N(D_{pp})D_{pp}^{3}} \quad \text{(eq. 1)}$$

In Eq. 1, $\rho_{pp}$ is the true density of NPs or soot aggregates, $\Phi$ is an empirical constant equal to 1.3 and related to the overlapping coefficient Cov previously defined in Brasil et al. (1999), $N_{pp}$ represents the number of primary particles composing the aggregate and $N(D_{pp})$ the number of primary particles within the size class $d_{Dpp}$. Major limitation of equation (1) is due to the number of primary particle composing aggregates analyzed on TEM images. In the present study, since we do not have access to TEM images of each samples, especially for those coming from literature, we have simplified equation (1) by assuming that soot aggregates generally present more than 50 primary particles, which is in good agreement with values reported in several studies (Köylü & Faeth, 1992; Ouf et al., 2008). Another major assumption associated to equation (1) consists in considering each primary particle in contact with only 2 other primary particles. This hypothesis is generally assumed to be relevant for nanoparticles aggregates formed mainly by diffusion (Brasil et al., 2001; Harada et al., 2006). Furthermore, assuming primary particles moderately polydispersed, in terms of diameter (geometric standard deviation lower than 1.8 as generally reported in literature, Bourrous et al., 2018), the count median diameter $\overline{D_{pp}}$ could be considered as a relevant descriptor to calculate surface and mass of the population. Then, according to previous assumptions, one could simplify equation (1) as follows:

$$S_{TEM}=\frac{6}{\rho_{sample}.\overline{D_{pp}}}\left[1-\Phi Cov\right] \quad \text{(eq. 2)}$$

Equation (2) is used for computing specific surface area, using bulk densities and overlapping coefficient previously reported (Bourrous et al., 2018; Ouf et al., 2019) or analyzed in the present study. Figure 2 presents the correlation between $S_{TEM}$ and $S_{BET}$ for samples produced under realistic combustion and fire conditions. The raw results are reported in tables 1 and 2. Uncertainties associated to $S_{TEM}$ have been computed by error propagation from equation (2) (see annex I for more details on the method). It corresponds to a mean relative uncertainty of 19%.

A relatively good agreement between $S_{TEM}$ and $S_{BET}$ is found for most of the samples produced by diffusion flames of hydrocarbons, oil or polymer fuels. Most samples denote TEM determined values in agreement with BET analysis within the +/- 20 % confidence interval previously reported by Bourrous et al. (2018) for a limited number of samples. Nevertheless, for certain samples produced during real scale fires, the specific surface area deduced by TEM analysis is overestimated compared to $S_{BET}$ method.

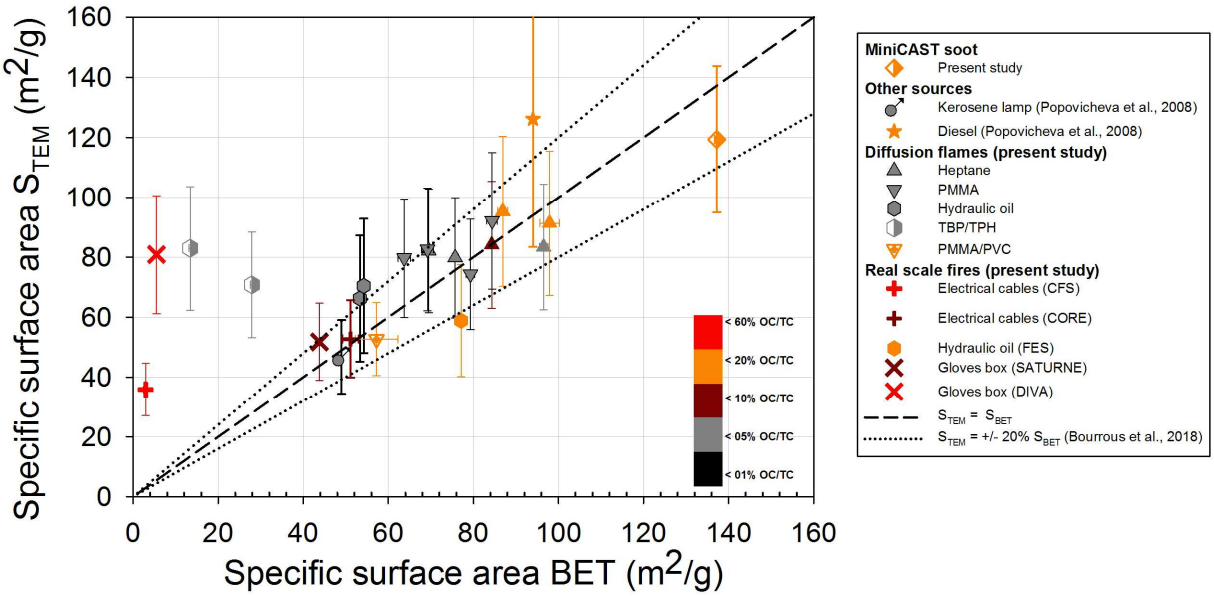


Figure 2: Parity graph between $S_{TEM}$, deduced from TEM analysis and computed according to equation 2, and $S_{BET}$ analysis

**<u>An attempt of generalization of the $S_{TEM}$ approach for unknown true density samples</u>**

As reported in figure 2, it must be noted that a significant amount of organic contents (more than 20%), sorbed on particles, can decrease the surface available for nitrogen adsorption and thus could provide lower $S_{BET}$. To confirm the impact of the OC content on the specific surface area, BET measurements have been performed on Heptane, PMMA and TBP/TPH combustion particles thermally outgassed at 105°C and 400°C. Mass loss has then been measured (and compared to the initial sample mass) and BET analysis performed on those post-treated samples. Figure 3 presents the factor of specific surface increase (ratio between the measured specific surface area values after heating with that determined for initially non-treated particles) as a function of the mass loss caused by heating treatment.

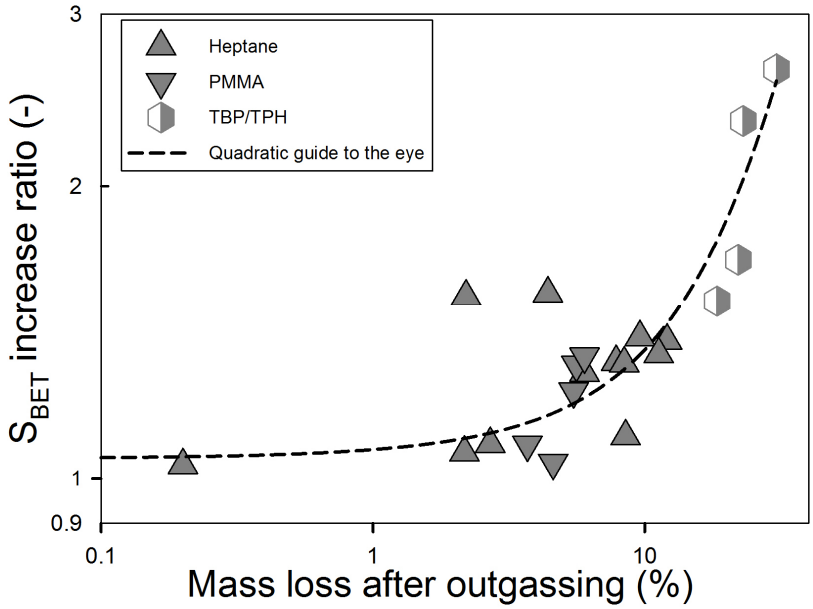


Figure 3: Increase of the specific surface area measured by BET with outgassing level (diffusion flames combustion conditions)

One could notice that specific surface area significantly increases as a function of mass loss (see the quadratic law presented in figure 3 as a guide to the eye). This confirms that the OC content has on the one hand an influence on the particle density (Bourrous et al. 2018) and on the other hand an influence on the available surface of those samples. For TBP/TPH, one must notice that, as previously reported by our team (Ouf et al., 2015), particles produced during combustion of such complex mixing of solvents, contain not only organic carbon, but also a significant amount of aqueous phase containing phosphoric acid $H_3PO_4$, in the form of a droplet formed at soot surface. In this case, developed surface of particles emitted during fire involving TBP/TPH will be reduced by water and $H_3PO_4$ sorption, explaining the significantly lower specific surface area measured by $S_{BET}$ as compared with $S_{TEM}$.

In consequence of Figure 3, it seems that computation of specific surface area from TEM analysis, as proposed by Bourrous et al. (2018) for nanostructured and soot samples, is a reliable approach. Furthermore, it presents the advantage to be applicable when the amount of mass of samples is hardly reachable. Nevertheless, in order to be fully predictable, such approach requires the true sample density as data input. Such property is generally measured using Helium pycnometry[1] and volume displacement methods such as ISO 787-23[2] and we have recently proposed an analysis of values reported within literature and experimentally for realistic conditions of production of combustion generated particles. In most cases, with these methods, at least 500 mg of powder is needed to perform a relevant true density analysis, and then one could suspect that, when specific surface area measurement is not possible due to a limited amount of sample, similarly true density will be also hardly measured. Nevertheless, and as demonstrated in Ouf et al. (2019), the effective density approach proposed by Yon et al., (2015) could be applied for measuring the true density of combustion generated aerosol, even for low mass or number concentrations.

We propose hereafter a simple approach for estimating the true sample density of combustion generated particles according to their composition. One must notice that, in the present study, sample density is associated to true density of the overall material composing aggregate and its coating. As recently demonstrated, true density of combustion emitted particles presents significantly different values ranging from nearly 1285 kg/m$^3$ to 2069 kg/m$^3$ and strongly depends on OC/TC ratio (Ouf et al., 2019). For taking into account such discrepancies, we

[1] https://www.astm.org/Standards/B923.htm
[2] https://www.iso.org/standard/5102.html

have fitted the experimental evolution, reported in Ouf et al., (2019), of true sample density as a function of OC/TC according to a simple exponential decay law:

$$\rho_{sample}=1234+882\exp(-0.083\ OC/TC), \qquad \text{(eq. 3)}$$

with $\rho_{sample}$ and OC/TC respectively expressed in kg/m$^3$ and in % (from 0 to 100 % of OC/TC).

Figure 4 presents the comparison between $S_{TEM}$, computed according to equations 2 and 3, and $S_{BET}$. Reasonable agreement could be noticed for samples denoting low (<5%) and moderate OC/TC content (<20%). On the other hand, as expected, specific surface area of samples denoting OC/TC content higher than 50% and metallic elements are in poor agreement with BET analysis. For such complex samples, knowledge of true sample density appears to be crucial for a realistic estimation of specific surface area. As an overall conclusion of this attempt of implementation of OC/TC within a TEM based specific surface area analysis method, present approach does not provide real improvement. Prediction of true density from eq. 3 does not enhance the agreement between $S_{TEM}$ and $S_{BET}$, highlighting the complexity of composition of particles emitted in case of fire and, in the same way, the limitation of such simple approach of analysis. Without any prior knowledge of soot composition and nature, use of equations 1, 2 and 3 for computing specific surface area must be considered with caution and must be limited to OC/TC ratio lower than 20%.

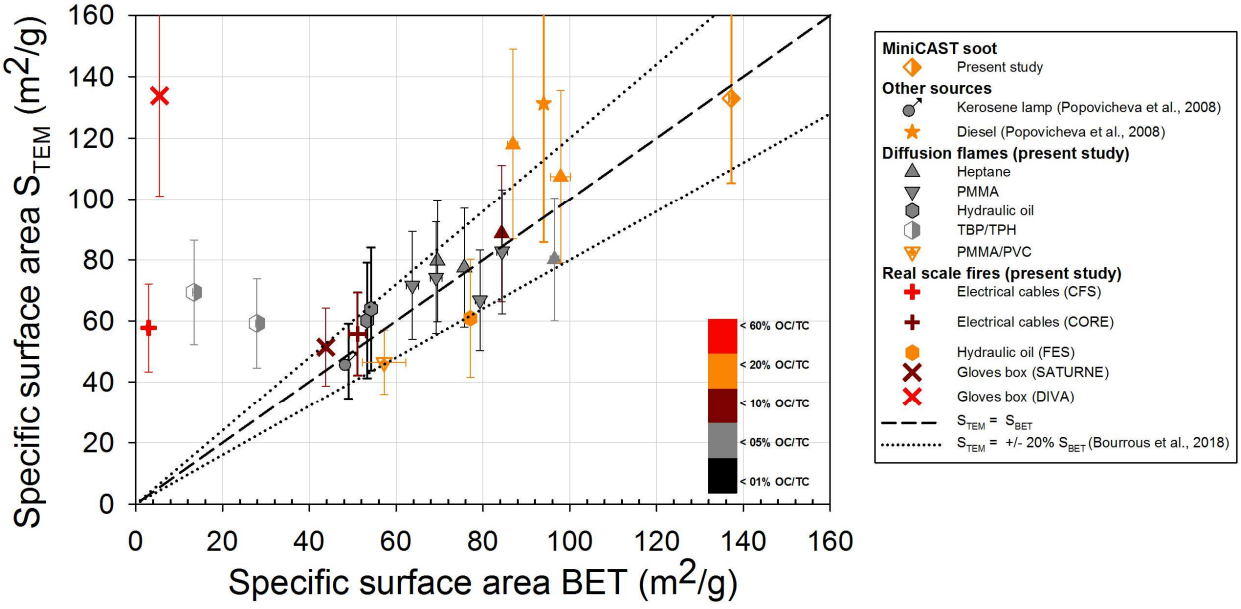


Figure 4: Parity graph between $S_{TEM}$, considering equations 2 and 3, and $S_{BET}$ analysis ($S_{BET}$ from 0 to 160 m²/g, corresponding to values reported in the present study for combustion emitted particles)

## Conclusions

Measurements of specific surface area, according to BET analysis, were experimentally conducted for soot and combustion emitted particles samples for more than 20 different combustion sources. Corresponding $S_{BET}$ are ranging from 3 m²/g to 98 m²/g. The impact of primary particle diameter is confirmed and, by outgassing organic containing samples, OC/TC ratio has been shown to have a strong influence. Specific surface area significantly decreases with increasing $D_{pp}$ and OC/TC. Based on TEM images analysis, a simple geometrical description of specific surface area, including overlapping between primary particles and true density of considered samples, is shown to give values in reasonable agreement with those obtained from BET analysis. Such agreement confirms that particles emitted under various combustion conditions could be assumed to be non-porous with homogeneous composition and considering the particles true density. Improvement of this previously proposed model is introduced, aiming to compute the true density of samples, when such information is not easily

reachable, as a function of OC/TC ratio. Comparison with BET values does not show a significant enhancement of the agreement of this modified model. This could probably be explained by the huge variety of soot considered in this study and denoting different true density and OC content.

**Acknowledgements**

Authors would like to acknowledge Guillaume Basso, Mickael Coutin, Vincent Cozar, Hugues Pretrel, Serge Pons and Pascal Zavaleta from the "Laboratoire d'Expérimentation des Feux" in Cadarache for providing soot samples emitted during large scale fire experiments. This work was partially done within the framework of the LIMA joint research program (The Interactions Media-Aerosol Laboratory) between the Institute for Radiological Protection and Nuclear Safety and the Reactions and Chemical Engineering Laboratory (LRGP) of the French National Centre for Scientific Research (CNRS).

**Table 1:** properties and specific surface area of carbon black commercial samples and soot from literature analysis

| Source | Fuel | OC/TC (%) | Diameter (nm) | $C_{ov}$ (-) | $\rho_{pp}$ (kg/m$^3$) | $S_{BET}$ (m$^2$/g) | Reference |
|---|---|---|---|---|---|---|---|
| Carbon black commercial samples | Flamruss LB 101 | 0.8[1] / 0.8[2] | 135.8 +/- 8.4 | 0 | 1717 +/- 49 | 24.4 +/- 0.08 | [1]Present study / [2](Saber et al., 2012) / [3](Ferge et al., 2006) / [4]supplier |
| | Printex 90 | 1.3[1] / 2.0[3] / 1[4] / 2[5] | 25.0 +/- 0.3 | | 1791 +/- 15 | 340 +/- 1.57 | |
| | Degussa S170 | 8.57* | 14.6 +/- 3.8 | | 1800[4] | 197.0 | (Ferraro et al., 2016) / [4]supplier |
| | Corax N110 | 1.31* | 13.8 +/- 4.0 | | | 122.4 | |
| | Corax N234 | 5.70* | 21.7 +/- 7.4 | | | 111.2 | |
| | Corax N326 | 4.68* | 24.7 +/- 9.6 | | | 58.7 | |
| | Corax N539 | 3.19* | 43.3 +/- 15.7 | | | 36.0 | |
| | Printex 25 | 0.9[4] | 49 | | 1878 +/- 15 | 51 | (Miroslawa Pawlyta, Rouzaud, & Duber, 2015) |
| | Printex 60 | 1[4] | 34 | | 1800[4] | 106 | |
| | Printex 90 | 1.3[1] / 2.0[3] / 1[4] / 2[5] | 19 | | 1791 +/- 15 | 336 | |
| | Colour Black FW 200 | 20[4] | 18 | | 1800[4] | 545 | |
| | Printex U | 5[4] | 36.9 +/- 9.4 | | | 97.24 | (Liu et al., 2010) |
| | Printex G | 0.7[4] / 1[5] | 30-60/51 | | | 43/30 | [5](Stoeger et al., 2005) |
| | Printex 90 | 1.3[1] / 2.0[3] / 1[4] / 2[5] | 12-17/14 | | 1791 +/- 15 | 272/300 | |
| | Thermal | 0.6 | 246 | | 1800[4] | 10 | (Popovicheva et al., 2008) |
| miniCAST burner | CAST1 | 16.2[6] | 26.5[6] ($\sigma_g$=1.36) | 0.11 +/- 0.10[6] | 1631 +/- 132 | 137.2 +/- 0.5[7] | [6](Soleiman Bourrous et al., 2018) / [7](Monge et al., 2010) |
| | SootH (High OC content) | 19 | 8-16 | | | 268 | (Stoeger et al., 2005) [8](Thomas et al., 2014) / [9](Wentzel et al., 2003) |
| | SootL (Low OC content) | 7 | 8-14 | | | 441 | |
| Spark discharge | ufCP | 17 | 7-12 | 0[8, 9] | 2150 | 807 | |
| | Palas | 0 | 6.6 | | | 308 | (Popovicheva et al., 2008) [8](Thomas et al., 2014) [9](Wentzel et al., 2003) |
| Kerosene in oil lamp | TC1 | 2.1 / 4 | 57 | 0.14 +/- 0.14¤ | 1834 +/- 187 | 49 | |
| Diesel engine | Diesel soot-in-oil sample | 16.15* | 25.4 +/- 15.2 (91.3%) 48.0 +/- 8.1 (8.7%) | 0.14 +/- 0.14¤ | 1525 +/- 361[10] | 94 | (Ferraro et al., 2016) [10](Park, Kittelson, & McMurry, 2004) |
| Candle | Candle soot | 3.5** | 20-50 | 0.14 +/- 0.14¤ | 1834 +/- 187 | 366 | (Qahtan et al., 2017) |

*Atomic percentage of elements others than N, C and H **TGA weight loss at 450°C in agreement with oxygen atomic percentage of 3.0% ¤ when not available, $C_{ov}$ was assumed as mean value of measured $C_{ov}$

**Table 2:** properties and bulk density of combustion emitted particles samples of present study

| Source | Production conditions | | | OC/TC (%) | Diameter (nm) | $C_{ov}$ (-) | $\rho_{pp}$ (kg/m$^3$) | $S_{BET}$ (m$^2$/g) | Reference |
|---|---|---|---|---|---|---|---|---|---|
| | Fuel | [$O_2$] | Scale | | | | | | |
| Diffusion Flames (cone calorimeter) | Heptane | 21% | Small | 4.4 +/- 2.3 | 35.1 +/- 1.3 | 0.13 +/- 0.15[6] | 1780 +/- 20[11] | 75.5 +/- 0.75 | Present study<br>[6](Soleiman Bourrous et al., 2018)<br>11(Mullins & Williams, 1987) |
| | | | Medium | 1.0 +/- 0.01 | 34.1 +/- 1.3 | | | 69.5 +/- 0.68 | |
| | | 19% | Small | 8.0 +/- 3.0 | 33.3 +/- 0.9 | | | 84.3 +/- 0.69 | |
| | | 17% | Small | 4.3 +/- 1.6 | 33.6 +/- 0.5 | | | 96.5 +/- 1.03 | |
| | | 15% | Small | 13.8 +/- 2.5 | 31.2 +/- 1.3 | 0.12 +/- 0.16[6] | | 97.9 +/- 2.29 | |
| | | | Medium | 17.6 +/- 6.6 | 29.9 +/- 0.9 | | | 86.9 +/- 1.18 | |
| | PMMA | 21% | Small | 3.5 +/- 1.4 | 39.9 +/- 0.8 | 0.14 +/- 0.14¤ | 1648 +/- 78 | 79.3 +/- 1.05 | |
| | | | Medium | 2.0 +/- 1.0 | 35.9 +/- 1.1 | | | 69.2 +/- 1.38 | |
| | | 18% | Small | 4.0 +/- 2.5 | 32.2 +/- 0.8 | | | 84.4 +/- 1.24 | |
| | | | Medium | 2.9 +/- 1.2 | 37.2 +/- 1.2 | | | 63.7 +/- 1.42 | |
| | Hydraulic oil | 21% | Small | 2.1 +/- 1.5 | 42.1 +/- 1.2 | 0.17 +/- 0.17 | 1665 +/- 164 | 53.3 +/- 1.10 | |
| | | 17% | Small | 3.1 +/- 3.2 | 38.6 +/- 1.1 | | | 54.2 +/- 1.18 | |
| | TBP/TPH | 21% | Small | 3.2 +/- 2.6† | 45.0 +/- 1.4 | 0.14 +/- 0.14¤ | 1534 +/- 78 | 27.9 +/- 0.33 | |
| | | 17% | Small | 4.2 +/- 3.4† | 38.4 +/- 1.0 | | | 13.4 +/- 0.28 | |
| | PMMA/PVC | - | Medium | 14.8 +/- 2.3 | 72.0[6] | 0.13 +/- 0.13[6] | 1315 +/- 82 | 57.2 +/- 5.0[6] | |
| Real scale fires | Electrical cables (CFS) | | | 55.3 +/- 2.8†† | 68.1 +/- 2.4 | 0.14 +/- 0.14¤ | 2000 +/- 60 | 2.94 +/- 0.5 | |
| | Electrical cable with PVC (CORE) | | | 8.4 +/- 1.0†† | 52.4 +/- 2.0 | 0.14 +/- 0.14¤ | 1768 +/- 39 | 51.1 +/- 1.9[6] | |
| | Hydraulic oil (FES) | | | 10.3 +/- 0.4 | 47.3[6] | 0.17 +/- 0.17[6] | 1665 +/- 164 | 77.1 +/- 1.3[6] | |
| | Gloves box (SATURNE) | | | 6.2 +/- 0.6 | 41.8[6] | 0.20 +/- 0.13[6] | 1749 +/- 82 | 43.8 +/- 0.1[6] | |
| | Gloves box (DIVA) | | | 48.1 +/- 3.4†† | 29.2 | 0.14 +/- 0.14¤ | 2069 +/- 35 | 5.48 | |

†Soot containing significant $H_3PO_4$ content ††Soot containing significant metal content ¤ when not available, $C_{ov}$ was assumed as mean value of measured $C_{ov}$

**References:**


Bau, S., Witschger, O., Gensdarmes, F., Rastoix, O., & Thomas, D. (2010). A TEM-based method as an alternative to the BET method for measuring off-line the specific surface area of nanoaerosols. *Powder Technology*, *200*(3), 190–201. http://doi.org/10.1016/j.powtec.2010.02.023

Bolstad-Johnson, D. M., Burgess, J. L., Crutchfield, C. D., Storment, S., Gerkin, R., & Wilson, J. R. (2000). Characterization of firefighter exposures during fire overhaul. *American Industrial Hygiene Association Journal*, *61*(5), 636–41. http://doi.org/10.1202/0002-8894(2000)061<0636:COFEDF>2.0.CO;2

Bourrous, S., Bouilloux, L., Ouf, F.-X., Lemaitre, P., Nerisson, P., Thomas, D., & Appert-Collin, J. C. (2016). Measurement and modeling of pressure drop of HEPA filters clogged with ultrafine particles. *Powder Technology*, *289*. http://doi.org/10.1016/j.powtec.2015.11.020

Bourrous, S., Ribeyre, Q., Lintis, L., Yon, J., Bau, S., Thomas, D., … Ouf, F. F.-X. (2018). A semi-automatic analysis tool for the determination of primary particle size, overlap coefficient and specific surface area of nanoparticles aggregates. *Journal of Aerosol Science*, *126*(February), 122–132. http://doi.org/10.1017/S0950268817001236.

Brasil, A. M., Farias, T. L., & Carvalho, M. G. (1999). A recipe for image characterization of fractal-like aggregates. *Journal of Aerosol Science*, *30*(10), 1379–1389. http://doi.org/10.1016/S0021-8502(99)00026-9

Brasil, A. M., Farias, T. L., Carvalho, M. G., & Koylu, U. O. (2001). Numerical characterization of the morphology of aggregated particles. *Journal of Aerosol Science*, *32*, 489–508. http://doi.org/10.1016/S0021-8502(00)00097-5

Cheung, S. C. ., Yuen, R. K. ., Yeoh, G. ., & Cheng, G. W. . (2004). Contribution of soot particles on global radiative heat transfer in a two-compartment fire. *Fire Safety Journal*, *39*(5), 412–428. http://doi.org/10.1016/j.firesaf.2004.03.004

Chow, J. C., Watson, J. G., Chen, L. W. A., Chang, M. C. O., Robinson, N. F., Trimble, D., & Kohl, S. (2007). The IMPROVE_A temperature protocol for thermal/optical carbon analysis: maintaining consistency with a long-term database. *Journal of the Air & Waste Management Association (1995)*, *57*, 1014–1023. http://doi.org/10.3155/1047-3289.57.9.1014

Dazon, C., Witschger, O., Bau, S., Payet, R., Fierro, V., & Jensen, K. A. (2017). On the equivalence between mass-specific surface area of powders and their aerosols and proposal of a new dustiness index for bulk nanomaterials Prediction and quantification of emissions and workers exposure during ceramic industrial processes. In *European Aerosol Conference* (p. 2017). Zurich,.

Ferge, T., Karg, E., Schröppel, A., Coffee, K. R., Tobias, H. J., Frank, M., … Zimmermann, R. (2006). Fast determination of the relative elemental and organic carbon content of aerosol samples by on-line single-particle aerosol time-of-flight mass spectrometry. *Environmental Science and Technology*, *40*(10), 3327–3335. http://doi.org/10.1021/es050799k

Ferraro, G., Fratini, E., Rausa, R., Fiaschi, P., & Baglioni, P. (2016). Multiscale Characterization of Some Commercial Carbon Blacks and Diesel Engine Soot. *Energy and Fuels*, *30*(11), 9859–9866. http://doi.org/10.1021/acs.energyfuels.6b01740

Gregg, S. J., & Sing, K. S. W. (1982). *Adsorption, surface area and porosity*. (A. P. Inc., Ed.) (Second Edi). London.

Gregory, W. S., Martin, R. A., Smith, P. R., & Fenton, D. E. (1982). Response of HEPA filters to simulated-accident conditions. http://doi.org/10.2172/5062853

Gustafsson, O., & Gschwend, P. M. (1997). Soot as a strong partition medium for polycyclic aromatic hydrocarbons in aquatic systems. *Molecular Markers in Environmental Geochemistry*, 365–381.

Gwaze, P., Schmid, O., Annegarn, H. J., Andreae, M. O., Huth, J., & Helas, G. (2006). Comparison of three methods of fractal analysis applied to soot aggregates from wood combustion. *Journal of Aerosol Science*, *37*(7), 820–838. http://doi.org/10.1016/j.jaerosci.2005.06.007

Harada, S., Tanaka, R., Nogami, H., & Sawada, M. (2006). Dependence of fragmentation behavior of colloidal aggregates on their fractal structure. *Journal of Colloid and Interface Science*, *301*(1), 123–129. http://doi.org/10.1016/j.jcis.2006.04.051

Hertzberg, T., & Blomqvist, P. (2003). Particles from fires - A screening of common materials found in buildings. *Fire and Materials*, *27*(6), 295–314. http://doi.org/10.1002/fam.837

Ishibashi, T., Tsuchino, S., Matsumoto, S., & Kasahara, F. (2014). Clogging of HEPA filters by soot during fire events in nuclear fuel cycle facilities. *Nuclear Technology*, *187*, 57–68.

Jonker, M. T. O., & Koelmans, A. A. (2002). Sorption of polycyclic aromatic hydrocarbons and polychlorinated biphenyls to soot and soot-like materials in the aqueous environment: Mechanistic considerations. *Environmental Science and Technology*, *36*(17), 3725–3734. http://doi.org/10.1021/es020019x

Köylü, Ü. Ö., & Faeth, G. M. (1992). Structure of overfire soot in buoyant turbulent diffusion flames at long residence times. *Combustion and Flame*, *89*(2), 140–156. http://doi.org/10.1016/0010-2180(92)90024-J

Liu, Y., Liu, C., Ma, J., Ma, Q., & He, H. (2010). Structural and hygroscopic changes of soot during heterogeneous reaction with O3. *Physical Chemistry Chemical Physics*, *12*, 10896–10903. http://doi.org/10.1039/c0cp00402b

Michelsen, H. A., Liu, F., Kock, B. F., Bladh, H., Boiarciuc, A., Charwath, M., … Suntz, R. (2007). Modeling laser-induced incandescence of soot: a summary and comparison of LII models. *Applied Physics B - Lasers and Optics*, *87*(3), 503–521. http://doi.org/10.1007/s00340-007-2619-5

Mocho, V. M., & Ouf, F. X. (2011). Clogging of industrial pleated high efficiency particulate air (HEPA) filters in the event of fire. *Nuclear Engineering and Design*, *241*(5), 1785–1794. http://doi.org/10.1016/j.nucengdes.2011.01.036

Monge, M. E., D'Anna, B., Mazri, L., Giroir-Fendler, A., Ammann, M., Donaldson, D. J., & George, C. (2010). Light changes the atmospheric reactivity of soot. *Proceedings of the National Academy of Sciences of the United States of America*, *107*(15), 6605–6609. http://doi.org/10.1073/pnas.0908341107

Motzkus, C., Chivas-Joly, C., Guillaume, E., Ducourtieux, S., Saragoza, L., Lesenechal, D., … Longuet, C. (2012). Aerosols emitted by the combustion of polymers containing nanoparticles. *Journal of Nanoparticle Research*, *14*(3), 1–17. http://doi.org/10.1007/s11051-011-0687-2

Mullins, J., & Williams, A. (1987). The optical properties of soot: a comparison between experimental and theoretical values. *Fuel*, *66*, 277–280. http://doi.org/10.1111/j.1365-263X.1994.tb00128.x

Ouf, F.-X., Bourrous, S., Fauvel, S., Kort, A., Lintis, L., Nuvoli, J., & Yon, J. (2019). True density of combustion emitted particles: A comparison of results highlighting the influence of the organic contents. *Journal of Aerosol Science*, *134*(April), 1–13. http://doi.org/10.1016/j.jaerosci.2019.04.007

Ouf, F.-X., Mocho, V.-M., Pontreau, S., Wang, Z., Ferry, D., & Yon, J. (2014). Clogging of industrial High Efficiency Particulate Air (HEPA) filters in case of fire: From analytical to large-scale experiments. *Aerosol Science and Technology*, *48*(9). http://doi.org/10.1080/02786826.2014.947022

Ouf, F.-X., Mocho, V.-M., Pontreau, S., Wang, Z., Ferry, D., & Yon, J. (2015). Physicochemical properties of aerosol released in the case of a fire involving materials used in the nuclear industry. *Journal of Hazardous Materials*, *283*, 340–349. http://doi.org/10.1016/j.jhazmat.2014.09.043

Ouf, F.-X., Vendel, J., Coppalle, A., Weill, M., & Yon, J. (2008). Characterization of Soot Particles in the Plumes of Over-Ventilated Diffusion Flames. *Combustion Science and Technology*, *180*(4), 674–698.

Ouf, F. X., Yon, J., Ausset, P., Coppalle, A., & Maillé, M. (2010). Influence of Sampling and Storage Protocol on Fractal Morphology of Soot Studied by Transmission Electron Microscopy. *Aerosol Science and Technology*, *44*(11), 1005–1017. http://doi.org/10.1080/02786826.2010.507228

Park, K., Kittelson, D. B., & McMurry, P. H. (2004). Structural properties of diesel exhaust particles measured by Transmission Electron Microscopy (TEM): Relationships to particle mass and mobility. *Aerosol Science and Technology*, *38*(9), 881–889. http://doi.org/10.1080/027868290505189

Pawlyta, M., Rouzaud, J.-N., & Duber, S. (2015). Raman microspectroscopy characterization of carbon blacks: Spectral analysis and structural information. *Carbon*, *84*, 479–490. http://doi.org/10.1016/j.carbon.2014.12.030

Pawlyta, M., Soble, B., & Liszka, B. (2018). Estimation of the chemical specific surface area of catalytic nanoparticles by TEM images analysis. *Journal of Achievements in Materials and Manufacturing Engineering*, *87*(1), 5–12. http://doi.org/10.1016/S0325-7541(13)70009-9

Petzold, A., Ogren, J. A., Fiebig, M., Laj, P., Li, S. M., Baltensperger, U., … Zhang, X. Y. (2013). Recommendations for reporting black carbon measurements. *Atmospheric Chemistry and Physics*, *13*(16), 8365–8379. http://doi.org/10.5194/acp-13-8365-2013

Pierce, J. B. M., & Moss, J. B. (2007). Smoke production, radiation heat transfer and fire growth in a liquid-fuelled compartment fire. *Fire Safety Journal*, *42*(4), 310–320. http://doi.org/10.1016/j.firesaf.2006.11.006

Popovicheva, O. B., Persiantseva, N. M., Tishkova, V., Shonija, N. K., & Zubareva, N. A. (2008). Quantification of water uptake by soot particles. *Environmental Research Letters*, *3*(2), 25009. http://doi.org/10.1088/1748-9326/3/2/025009

Qahtan, T. F., Gondal, M. A., Alade, I. O., & Dastageer, M. A. (2017). Fabrication of Water Jet Resistant and Thermally Stable Superhydrophobic Surfaces by Spray Coating of Candle Soot Dispersion. *Scientific Reports*, *7*(1), 1–7. http://doi.org/10.1038/s41598-017-06753-4

Rhodes, J., Smith, C., & Stec, A. A. (2011). Characterisation of soot particulates from fire retarded and nanocomposite materials, and their toxicological impact. *Polymer Degradation and Stability*, *96*(3), 277–284. http://doi.org/10.1016/j.polymdegradstab.2010.07.002

Saber, A. T., Jensen, K. A., Jacobsen, N. R., Birkedal, R., Mikkelsen, L., Møller, P., … Vogel, U. (2012). Inflammatory and genotoxic effects of nanoparticles designed for inclusion in paints and lacquers. *Nanotoxicology*, *6*(5), 453–71. http://doi.org/10.3109/17435390.2011.587900

Schmid, O., & Stoeger, T. (2016). Surface area is the biologically most effective dose metric for acute nanoparticle toxicity in the lung. *Journal of Aerosol Science*, *99*, 133–143. http://doi.org/10.1016/j.jaerosci.2017.09.017

Sing, K. S. W. (1985). Reporting physisorption data for gas/solid systems with special reference to the determination of surface area and porosity (Recommendations 1984). *Pure and Applied Chemistry*, *57*(4), 603–619. http://doi.org/10.1351/pac198557040603

Steiner, S., Bisig, C., Petri-Fink, A., & Rothen-Rutishauser, B. (2016). Diesel exhaust: current knowledge of adverse effects and underlying cellular mechanisms. *Archives of Toxicology*, *90*(7), 1541–1553. http://doi.org/10.1007/s00204-016-1736-5

Stoeger, T., Reinhard, C., Takenaka, S., Schroeppel, A., Karg, E., Ritter, B., … Schulz, H. (2005). Instillation of Six Different Ultrafine Carbon Particles Indicates a Surface Area Threshold Dose for Acute Lung Inflammation in Mice. *Environmental Health Perspectives*, *114*(3), 328–333. http://doi.org/10.1289/ehp.8266

Thomas, D., Ouf, F. X., Gensdarmes, F., Bourrous, S., & Bouilloux, L. (2014). Pressure drop model for nanostructured deposits. *Separation and Purification Technology*, *138*, 144–152. http://doi.org/10.1016/j.seppur.2014.09.032

Wang, X., Zhou, H., Arnott, W. P., Meyer, M. E., Taylor, S., Firouzkouhi, H., … Watson, J. G. (2019). Characterization of smoke for spacecraft fire safety. *Journal of Aerosol Science*, *136*(June), 36–47. http://doi.org/10.1016/j.jaerosci.2019.06.004

Wentzel, M., Gorzawski, H., Naumann, K. H., Saathoff, H., & Weinbruch, S. (2003). Transmission electron microscopical and aerosol dynamical characterization of soot aerosols. *Journal of Aerosol Science*, *34*(10), 1347–1370. http://doi.org/10.1016/S0021-8502(03)00360-4

Yon, J., Bescond, A., & Ouf, F.-X. (2015). A simple semi-empirical model for effective density measurements of fractal aggregates. *Journal of Aerosol Science*, *87*, 28–37. http://doi.org/10.1016/j.jaerosci.2015.05.003

## Annex I: computation of uncertainty associated to specific surface area determined by TEM images analysis

- The uncertainty $u(S_{TEM})$ associated to the specific surface area $S_{TEM}$ determined by TEM analysis and the Bau et al.'s model (2010) is computed according to the variances' propagation law:

$$S_{TEM}=\frac{6}{\rho_{pp}.D_{pp}}[1-\Phi.C_{ov}], \quad \text{(eq. AI-1)}$$

$$[u(S_{TEM})]^2=\frac{d^2S_{TEM}}{d\rho_{pp}^2}.\left[u\left(\rho_{pp}\right)\right]^2+\frac{d^2S_{TEM}}{dD_{pp}^2}.\left[u\left(D_{pp}\right)\right]^2+\frac{d^2S_{TEM}}{dC_{ov}^2}.[u(C_{ov})]^2, \quad \text{(eq. AI-2)}$$

$$\frac{d^2S_{TEM}}{d\rho_{pp}^2}=\left[-\frac{6}{\rho_{pp}^2.D_{pp}}.(1-\Phi.C_{ov})\right]^2, \quad \text{(eq. AI-3)}$$

$$\frac{d^2S_{TEM}}{dD_{pp}^2}=\left[-\frac{6}{\rho_{pp}.D_{pp}^2}.(1-\Phi.C_{ov})\right]^2, \quad \text{(eq. AI-4)}$$

$$\frac{d^2S_{TEM}}{dC_{ov}^2}=\left[-\frac{6.\Phi}{\rho_{pp}.D_{pp}}\right]^2. \quad \text{(eq. AI-5)}$$

- The uncertainty associated to the overlapping coefficient $u(C_{ov})$ is computed according to the variances' propagation law applied to the definition of $C_{ov}$:

-

$$C_{ov}=\xi_1.C_{ov,\ p}-\xi_2, \quad \text{(eq. AI-6)}$$

$$[u(C_{ov})]^2=\frac{d^2C_{ov}}{d\xi_1^2}.\left[u\left(\xi_1\right)\right]^2+\frac{d^2C_{ov}}{dC_{ov,p}^2}.\left[u\left(C_{ov,\ p}\right)\right]^2+\frac{d^2C_{ov}}{d\xi_2^2}.\left[u\left(\xi_2\right)\right]^2, \quad \text{(eq. AI-7)}$$

$$[u(C_{ov})]^2=\left[C_{ov,\ p}\right]^2.\left[u\left(\xi_1\right)\right]^2+\xi_1^2.\left[u\left(C_{ov,\ p}\right)\right]^2+\left[u\left(\xi_2\right)\right]^2, \quad \text{(eq. AI-8)}$$

with $\xi_1 = 1.1 + 0.1$ and $\xi_2 = 0.2 + 0.02$.

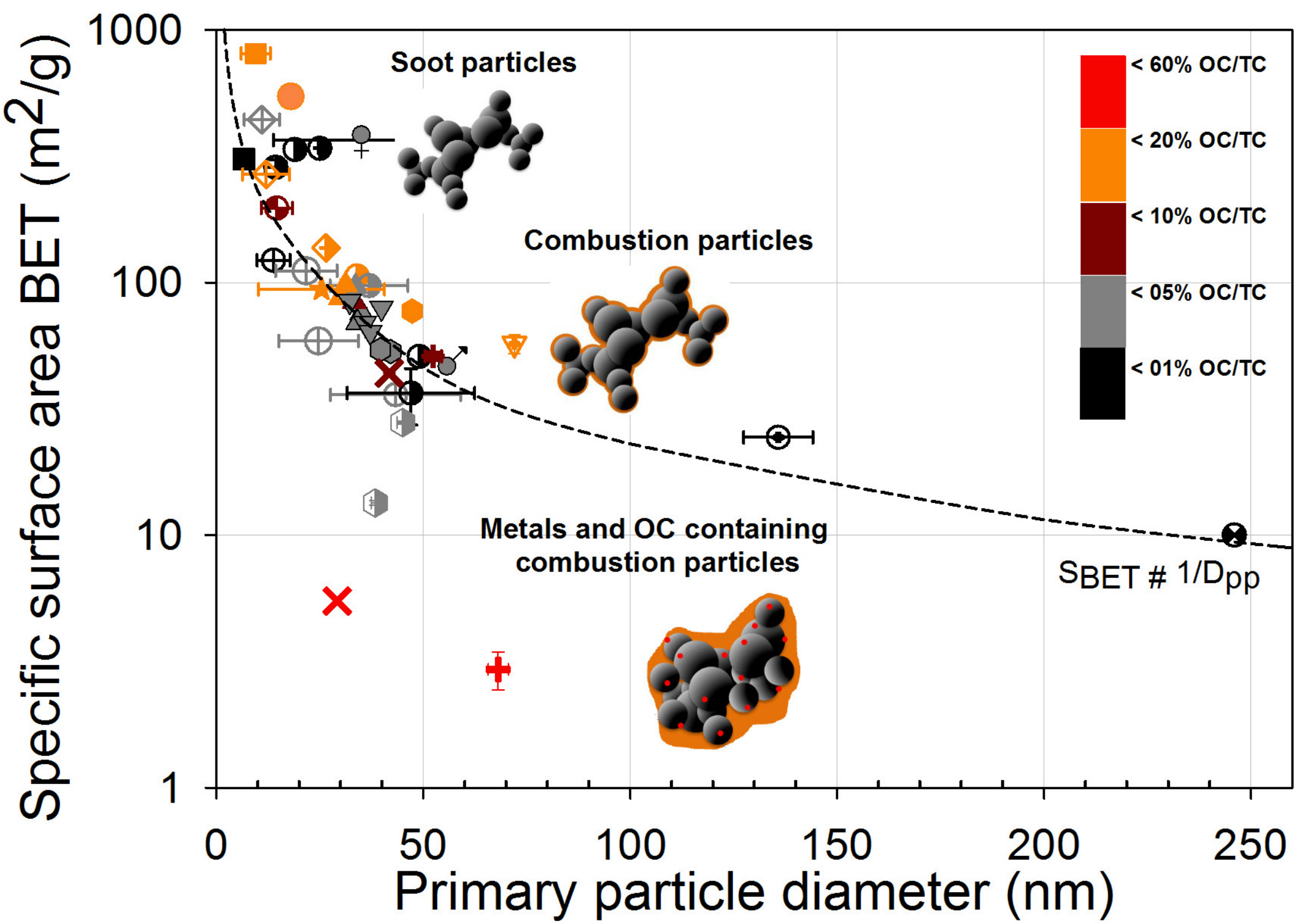
Specific surface area BET (m2/g)
1000
100
10
1
0
50
100
150
200
250
Primary particle diameter (nm)
Soot particles
Combustion particles
Metals and OC containing combustion particles
SBET # 1/Dpp
< 60% OC/TC
< 20% OC/TC
< 10% OC/TC
< 05% OC/TC
< 01% OC/TC